



Published in final edited form as:

*Brain Stimul.* 2020 ; 13(6): 1521–1523. doi:10.1016/j.brs.2020.08.005.

## Cerebellar tDCS consistency and metabolite changes: A recommendation to decrease barriers to replicability

**Alexandra B. Moussa-Tooks<sup>1</sup>,**

Psychological & Brain Sciences, Indiana University, Bloomington, IN, USA

Program in Neuroscience, Indiana University, Bloomington, IN, USA

**Leah P. Burroughs<sup>1</sup>,**

Psychological & Brain Sciences, Indiana University, Bloomington, IN, USA

**Abinand C. Rejimon,**

Psychological & Brain Sciences, Indiana University, Bloomington, IN, USA

**Hu Cheng,**

Psychological & Brain Sciences, Indiana University, Bloomington, IN, USA

Program in Neuroscience, Indiana University, Bloomington, IN, USA

**William P. Hetrick<sup>\*</sup>**

Psychological & Brain Sciences, Indiana University, Bloomington, IN, USA

Program in Neuroscience, Indiana University, Bloomington, IN, USA

Department of Psychiatry, Indiana University School of Medicine, Indianapolis, IN, USA

---

### Dear Editor,

Although transcranial direct current stimulation (tDCS) has shown promise in the literature for psychiatric and neurological conditions, the effects of cerebellar tDCS have proven variable and difficult to replicate [1]. Possible reasons for these replication issues include (1) gross individual difference characteristics (e.g., skin and skull thickness at the back of the head and neck, cerebellar morphology, etc.) that cause variability in conductivity based on tissue types [2] and structural variance [3] and (2) the complex cytoarchitecture of the cerebellum, particularly due to its intricate folds, high density and variety of cell types, and the prominence of inhibitory neurons, Purkinje cells [4]. Indeed, both field [5] and neuronal [6] orientation have been implicated in tDCS efficacy, such that modulation of signal transduction is dependent on homogenous populations of cells being oriented in the same direction, which is less likely to occur when grossly stimulating the cerebellum.

---

This is an open access article under the CC BY-NC-ND license (<http://creativecommons.org/licenses/by-nc-nd/4.0/>).

<sup>\*</sup>Corresponding author. 1101 E. 10th St. Bloomington, IN, 47405, USA. whetrick@indiana.edu (W.P. Hetrick).

<sup>1</sup>Both authors contributed equally to this work.

Declaration of competing interest

All authors declare that they have no conflicts of interest.

Accordingly, we conducted a preliminary study, in which all procedures were approved by the Indiana University Institutional Review Board, to begin addressing these considerations and propose a recommendation to the field to assuage these particular barriers to replication.

Twenty-five healthy participants (18 females, 7 males; mean age = 18.4 years [standard deviation = 0.7 years]) were recruited from the Indiana University Department of Psychological and Brain Sciences undergraduate participant pool. Exclusion criteria were consistent with a previously published study (cf. [7]), with additional criteria of contraindication for magnetic resonance scanning (i.e., metallic implants, etc.). After providing written informed consent, participants completed a scanning session that included anatomical T1 (3T Siemens Tim-Trio MR; high-resolution T1-weighted anatomical images [sagittal plane MP-RAGE sequence: TR = 1.8 s; TE = 2.67 ms; inversion time = 0.9 s; flip angle 9°; imaging matrix = 256 × 256; 192 slices; voxel size = 1 × 1 × 1 mm<sup>3</sup>]) and magnetic resonance spectroscopy (MRS) acquisition (voxel [2 × 2 × 2 cm<sup>3</sup>] positioned posteriorly in the superficial left cerebellum using midline sagittal T1 image placed [Fig. 1A]; nine 4-min single-voxel MRS acquisitions [two baseline, five tDCS (active or sham), and two recovery measures]; PRESS sequence [TR/ TE = 2000/30 ms, bandwidth = 2000 Hz, 2048 data points, 120 measurements] and subsequent water reference scan [8 averages]; cf [8]. for fully detailed methods including shimming procedures and data exclusion criteria) with simultaneous cerebellar tDCS (administered in accord with previously published methods (cf. [7]); 1.5 mA sham or active [cathode placed over the left cerebellar region [3 cm lateral to the inion] and the anode placed over the ipsilateral buccinator muscle (Fig. 1B)] stimulation beginning at the start of the third block of MRS acquisition and concluding at the termination of the seventh block of MRS acquisition for a total of 20 minutes of continuous stimulation).

### **Is there consistency of electrical signal transduction despite individual variability in gross anatomical features, including cerebellar morphology?**

Open-source computational modeling pipelines were utilized to model the electric field distribution and intensity for each participant (n = 25). First, ROAST [2] (version 2.7) was used to model whole brain electric field distribution during active stimulation (electrodes placed at sites I1 and Exx25 [10/ 05 system]; Fig. 1B). Within ROAST, the CLOS pipeline was then used to extract lobule-specific electric field data (Fig. 1C) [9]. Lobule-specific consistency of field intensity across participants was moderate (Fig. 1D; two-way mixed effects ICC = 0.762, 95% CI = 0.656 to 0.862, F(24,648) = 90.442, *p* < 0.001).

Encouragingly, modeling findings suggested that all participants received some quantity of stimulation and that peak electric field strength occurred within the same cerebellar lobules across participants (left lobules VII and VIII, primarily; Fig. 1D).

### **To what extent does neural modulation, as assessed via changes in key metabolites, vary by predicted stimulation intensity?**

MRS data from thirteen participants (n = 5 sham, 8 active) was processed and analyzed with LCModel (<http://www.sprovencher.com/>, version 6.2-0R) as described previously by our group (cf. [8]). Key metabolites were chosen for analysis due to reliability of their signal and/or relevance to the cerebellar literature: glutamate (Glu), pooled glutamate and

glutamine (Glx), total *N*-acetylaspartate (tNAA: *N*-acetylaspartate and *N*-acetylaspartylglutamate), and total creatine (tCr: creatine and phosphocreatine) [10]. A 9 (time) by 3 (stimulation [active high vs. active low vs. sham]) repeated measures ANOVA was used to test the impact of stimulation intensity on metabolite modulation. Field mapping data was used to divide those receiving active stimulation ( $n = 8$ ) into high ( $>0.14 \text{ mV/m}^3$ ;  $n = 4$ ) and low ( $<0.14 \text{ mV/m}^3$ ;  $n = 4$ ) intensity groups based on the average intensity from left cerebellar lobules VIIb, VIIIa, VIIIb, and IX. These lobules were selected a priori based on the placement of the spectroscopy voxel (Fig. 1A). There was a significant main effect of stimulation (low, high, and sham) on tCr between the subgroups (Fig. 1E;  $F(2,10) = 16.836$ ,  $p = 0.05$ ,  $\eta p^2 = 0.45$ ). LSD-corrected post-hoc pair-wise comparisons indicated lower tCr ( $p = 0.02$ ) and Glu ( $p = 0.044$ ; Fig. 1F) concentrations in individuals with high intensity stimulation compared to low intensity stimulation, though these groups still did not differ from the sham group. A main effect of time was observed for tCr ( $F(8,80) = 3.575$ ,  $p = 0.001$ ,  $\eta p^2 = 0.263$ ) and Glu ( $F(8,80) = 2.409$ ,  $p = 0.022$ ,  $\eta p^2 = 0.194$ ) metabolites with no stimulation by time interaction effect. Thus, tDCS-related metabolite changes, for tCr specifically, may be related to the strength of the electric field induced at the region of interest. Potential modulation of tCr is particularly interesting due to creatine's role in ATP synthesis in the central nervous system, its high concentration in the cerebellum compared to cerebrum, and its relevance to clinical disorders such as cerebellar ataxia [10,11].

Taken together, these findings suggest that individual differences at the gross anatomical level may contribute to differential distributions of the induced electric field during stimulation protocols, which may further impact the ability to modulate cerebellar signaling. Though the sample size is small, this work is a critical first-step towards understanding the lack of replicability across cerebellar tDCS studies.

It is highly recommended that the ROAST [2] and CLOS [9] modeling pipelines are leveraged to more precisely target cerebellar sub-structures (e.g., lobules). Determining optimal electrode placement for an individual participant, if modulation of a certain a priori target structure is desired, will likely be more useful for replication than the use of a single, standard scalp-based electrode montage that is applied across all participants. The 'target' function embedded in the ROAST pipeline could be used for such a purpose [2]. Additionally, future studies may consider adjusting the administered current on a per subject basis to better standardize the strength of stimulation at a target site using MRI-based or MRI-free estimation methods [12].

## Acknowledgments

We wish to thank the IU Bloomington Imaging Research Facility staff and scanning technicians. We also wish to thank Zeynab Rezaee and Dr. Anirban Dutta for their assistance and sharing their scripts for the CLOS pipeline.

### Funding

This work was supported by the National Institutes of Health (T32 MH103213 to WPH and ABM; R01 MH074983, R01 DA048012, and R21 MH118617 to WPH; F31 MH119767 to ABM) and Indiana Clinical and Translational Sciences Institute (TL1 TR001107 and UL1 TR001108 to ABM).

## References

- [1]. Ferrucci R, Bocci T, Cortese F, Ruggiero F, Priori A. Cerebellar transcranial direct current stimulation in neurological disease. *Cerebellum Ataxias* 2016;3(1):16. [PubMed: 27595007]
- [2]. Huang Y, Datta A, Bikson M, Parra LC. Realistic vOlumetric-Approach to Simulate Transcranial Electric Stimulation d ROAST d a fully automated open-source pipeline. *J Neural Eng* 2019;16(5):56006.
- [3]. Steele CJ, Chakravarty MM. Gray-matter structural variability in the human cerebellum: lobule-specific differences across sex and hemisphere. *Neuroimage* 2018;170:164e73.
- [4]. Rahman A, Toshev PK, Bikson M. Polarizing cerebellar neurons with transcranial direct current stimulation. *Clin Neurophysiol* 2014;125(3):435e8. [PubMed: 24176296]
- [5]. Lopez L, Chan CY, Okada YC, Nicholson C. Multimodal characterization of population responses evoked by applied electric field in vitro: extracellular potential, magnetic evoked field, transmembrane potential, and current-source density analysis. *J Neurosci* 1991;11(7):1998e2010.
- [6]. Liu A, Voroslakos M, Kronberg G, Henin S, Krause MR, Huang Y, et al. Immediate neurophysiological effects of transcranial electrical stimulation. *Nat Commun* 2018;9(1):5092. [PubMed: 30504921]
- [7]. Mitroi J, Burroughs LP, Moussa-Tooks AB, Bolbecker AR, Lundin NB, O'Donnell BF, et al. Polarity- and intensity-independent modulation of timing during delay eyeblink conditioning using cerebellar transcranial direct current stimulation. *Cerebellum* 2020;19:383e91.
- [8]. Newman SD, Cheng H, Schnakenberg Martin A, Dydak U, Dharmadhikari S, Hetrick W, et al. An investigation of neurochemical changes in chronic cannabis users. *Front Hum Neurosci* 2019;13.
- [9]. Rezaee Z, Dutta A. Cerebellar lobules optimal stimulation (CLOS): a computational pipeline to optimize cerebellar lobule-specific electric field distribution. *Front Neurosci* 2019;13:266. [PubMed: 31031578]
- [10]. Pouwels PJ, Frahm J. Regional metabolite concentrations in human brain as determined by quantitative localized proton MRS. *Magn Reson Med* 1998;39(1):53e60. [PubMed: 9438437]
- [11]. Harno H, Heikkinen S, Kaunisto MA, Kallela M, Haekkinen A-M, Wessman M, et al. Decreased cerebellar total creatine in episodic ataxia type 2: a 1H MRS study. *Neurology* 2005;64(3):542e4. [PubMed: 15699392]
- [12]. Caulfield KA, Badran BW, Li X, Bikson M, George MS. Can transcranial electrical stimulation motor threshold estimate individualized tDCS doses over the prefrontal cortex? Evidence from reverse-calculation electric field modeling. *Brain Stimul* 2020;13(4):1150e2.

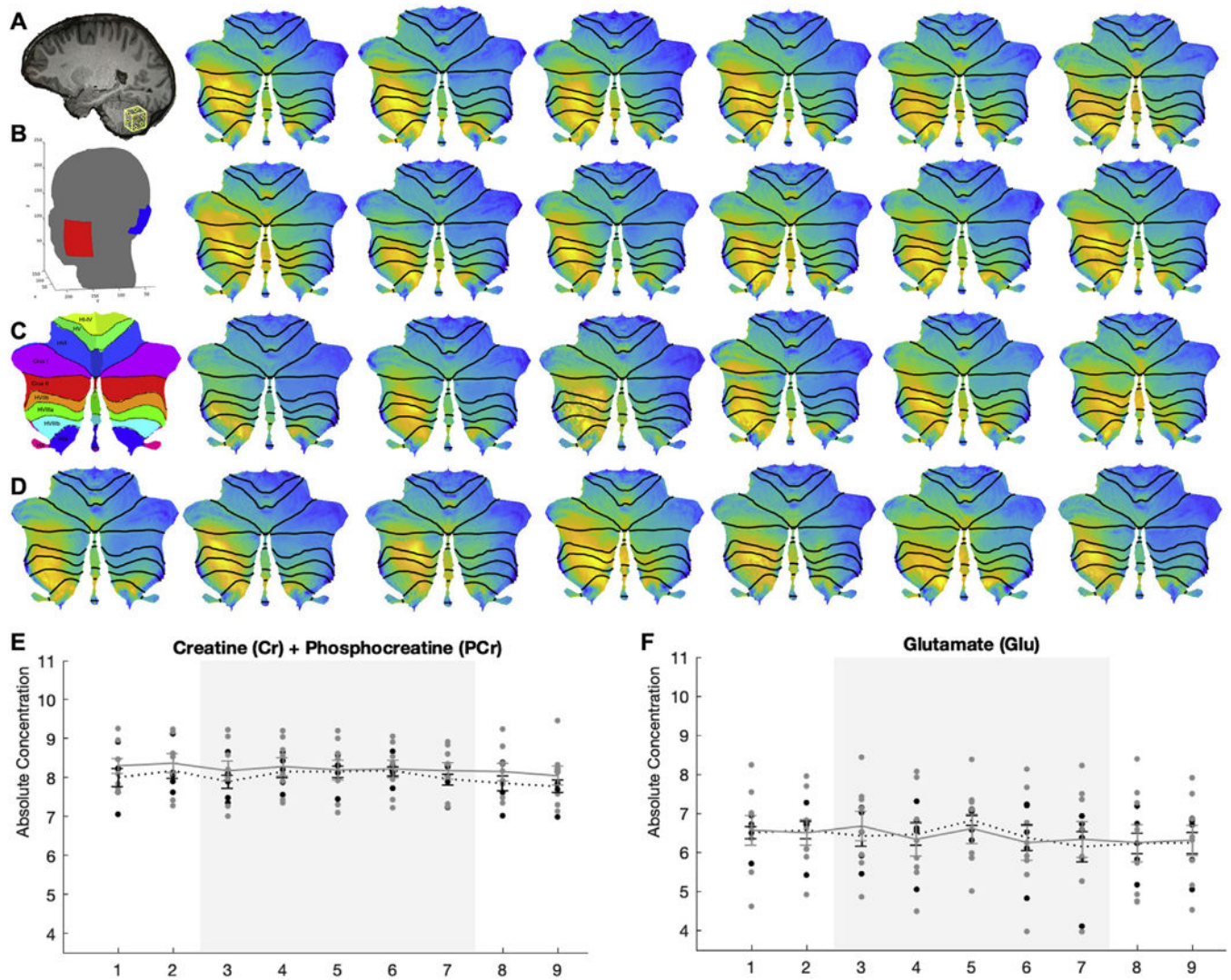


**Fig. 1.**

(A) Sagittal view of brain with spectroscopy voxel positioned in the cerebellum. (B) Electrode montage used for ROAST indicating scalp placement of electrodes. (C) Diagram of cerebellar lobules in flatmap (cf. Diedrichsen & Zotow, 2015, *PLoS One*). (D) Individual cerebellar flatmaps displaying standardized electric field magnitudes. (E) Absolute concentrations of cerebellar total Creatine and (F) Glutamate in active (black dots) and sham (grey dots) stimulation groups across each 4-min spectroscopy acquisition block (x-axis). Grey shading indicates the period of active stimulation administration.